Recoil distance lifetime measurements in ^{146}Sm

S. Rozak,* E. G. Funk, and J. W. Mihelich
Department of Physics, University of Notre Dame, Notre Dame, Indiana 46556
(Received 29 October 1981)

Recoil-distance lifetime measurements of levels in ^{146}Sm have been carried out using the (^{11}B,4n) reaction at 54 MeV on natural La targets evaporated on gold. The data were analyzed using a computer code which treats complex cascade feeding in a rigorous formalism. The following lifetimes have been measured (energy is in keV and spin parity are in parentheses): 1811.5(6$^+$), 125^{+140}_{-70} ps ; 2600.3(7$^-$), 16±6 ps; 2737.1(8$^+$), 16.4±6.0 ps; 2797.6(9$^-$), $1.20^{+0.29}_{-0.19}$ ns; 3354.5(9$^-$), 39^{+7}_{-6} ps; 3783.5(11$^-$), 15^{+6}_{-5} ps; 4091.2(11$^-$), $7.1^{+2.1}_{-1.9}$ ps; 4628.8(13$^-$), $7.6^{+3.3}_{-2.9}$ ps. Lifetimes have also been measured for the 747.2(2$^+$), 1381.2(4$^+$), and 4461.4(12$^-$) states but with considerably less precision. The results support the interpretation of the yrast odd-spin negative parity states (3$^-$ through 11$^-$) as being described by an octupole phonon coupled to the 0$^+$ through 8$^+$ yrast even-spin, positive-parity "ground-state band" states. The results for the 2$^+$ through 8$^+$ states are compared to calculations of the interacting boson approximation model and cluster-vibrator model. Both models are not inconsistent with the observed transition probabilities up to the 6$^+$→4$^+$ transition, but fail to reproduce that for the 8$^+$→6$^+$ transition. Our results support spin-parity arrangements of 12$^-$ and 13$^-$ for the 4461 and 4629 keV states, respectively.

[NUCLEAR REACTIONS ^{139}La(^{11}B,4n), E=54 MeV; measured recoil-distance Doppler shift. ^{146}Sm levels, deduced lifetimes, reduced transition probabilities. Ge(Li) detectors, plunger.]

I. INTRODUCTION

The transitional nuclei in the mass region $A \sim 150$ have been the subject of considerable investigation. In particular the samarium isotopes have been extensively studied since the accessible nuclides span the region from below the $N=82$ closed shell (^{144}Sm) to strongly deformed nuclei with $N \approx 92$.

The level structure of the nuclide ^{146}Sm (with 62 protons and 84 neutrons) cannot be interpreted in terms of simple collective models as this nuclide shows neither clear vibrational nor rotational structure. It is also only a few nucleons removed from ^{146}Gd which has 64 protons and 82 neutrons and exhibits doubly magic shell structure effects. Clearly a better understanding of ^{146}Sm is of considerable interest.

The level structure of ^{146}Sm below 5 MeV has been reasonably well established by Singh and Johns,[1] King *et al.*,[2] and Kownacki *et al.*,[3] although some ambiguities do exist. In the present investigation, the recoil distance method has been employed in a study of the lifetimes for several states in ^{146}Sm. The experimental results are compared to predictions of the cluster-vibrator model (CVM) which treats collective and particle degrees of freedom. In the framework of this model, Van den Berghe[4] has calculated wave functions for the lowest lying states in ^{146}Sm. The experimental results are also compared to predictions of the interacting boson approximation (IBA) model of Arima and Iachello.[5]

During the course of this work a new algorithm for describing arbitrarily complex cascade feeding has been developed. This algorithm is briefly described in Appendix A. A computer code PLUNGER[6] has been written incorporating this algorithm and several other corrections commonly applied to recoil distance method (RDM) data. PLUNGER has been written as the function (FCN) subroutine for the chi-squared minimization program MINUIT[7] which is capable of extracting errors for the variable parameters even when those parameters are strongly correlated.

II. EXPERIMENTAL PROCEDURE

The nucleus ^{146}Sm was studied using the reaction ^{139}La(^{11}B,4n) at 54 MeV with beams produced in the Notre Dame three-stage FN tandem accelerator.

The maximum recoil velocity for this reaction is 0.75% of c but this is reduced to an average of 0.6% of c due to energy loss and angle straggling in the target.

Our recoil-distance (plunger) apparatus permits target-stopper separations of from $\approx 10\,\mu$m to 5 mm, with a reproducibility of the order of 1 μm. The motion of the stage is by deflection of parallel leaf springs so that there is no play associated with rolling and sliding. A thrust bearing transmits the motion to the stage and backlash is practically eliminated. The target foil and recoil stopper are mounted on boron nitride insulators so that the capacitance between target and stopper may be monitored continuously. Because there is no room for a guard ring in this design, the elastance ($1/C$) is not directly proportional to distance, but it is a straightforward matter to determine the necessary correction.

The La targets were typically 0.23 to 0.27 mg/cm^2 thick and evaporated directly onto gold backings 1 mg/cm^2 thick. The detector was a coaxial Ge(Li) detector of 90 cm^3 active volume positioned 6 cm from the target and at 0° relative to the beam. The stopper foil was a 1 mg/cm^2 thick gold foil. For some of the data the foils were aligned by visual inspection. For later runs, they were aligned using the "optical lever" technique, described in Appendix B. The minimum target-stopper separation varied from 10 to 25 μm; the relatively large minimum separations were due mainly to imperfections along the rim of some of the foils used and much less so to foil misalignment.

Owing to the mixture of lifetimes involved, data were taken at 31 foil separation distances and in four separate experiments using three different target foils. Data were taken as singles spectra with no coincidence requirement imposed. When necessary the foil separation distances were scaled by the ratio of measured average recoil velocities to account for the roughly 15% variation in the target thicknesses from foil to foil.

In order to measure the background gamma rays coming from the reactions with the gold foils one run was taken with no La target foil but with gold foils used both for backing and stopper. When necessary this information was used to correct the areas of the full energy peaks of the gamma rays of interest.

The Doppler-shifted gamma rays were fitted using a line shape analysis based on the Blaugrund formalism.[8] The unshifted and shifted gamma rays were fitted with as few as three free parameters by requiring the Doppler-shifted component to conform to the theoretical shape and position calculated by doing a numerical integration over the target to get the velocity distribution and convoluting this into the gamma-ray line shape obtained from the shape of the unshifted component. The effective target thickness was varied slightly to produce velocity distributions that fit the peak shapes in the "clean" portions of the spectrum and the same parameters were then used to fit peaks that were not as well resolved or were parts of multiplets.

Lifetime information was extracted from the raw data using the conventional method of defining a quantity R which is the ratio of the unshifted intensity I_u to the sum of the unshifted and shifted intensities

$$R=\frac{I_u}{I_u+I_s}\ .$$

The lifetimes and other parameters were varied to reproduce the behavior of this ratio R versus the foil separation D.

The data were analyzed using the RDM data analysis program, PLUNGER, with cascade feeding included but with no higher order corrections since the statistical precision did not allow us to see effects of this magnitude. Estimates were made of the magnitude of these effects using the code PLUNGER and these estimates indicated that the dominant effect was cascade feeding with the next most important being the effect of target thickness. When corrections due to target thickness were included, the chi-squared fits improved by as much as 5% but did not appreciably affect the fitted lifetimes.

Owing to the strong correlations among the lifetimes caused by the strong cascade feeding, errors were extracted using the capabilities of the chi-squared minimization program MINUIT which accesses the FCN subroutine in PLUNGER.

III. RESULTS

For the RDM analysis the adopted level scheme was that given in Ref. 2 with the relative intensities of the strongest transitions determined by averaging the intensities measured in our 31 separate spectra and correcting these approximately for angular distribution effects using the angular distribution coefficients given in Ref. 2. We observe all of the strong transitions reported by King *et al.*[2] (those with relative intensities greater than about 4%) and

the relative intensities agree fairly well for the lower spin states ($I \leq 8$). We populate the higher spin states more strongly, as is expected with a heavier projectile.

For the analysis the transition intensities were generally kept fixed at their measured values. In some cases, the 430 keV ($6^+ \rightarrow 4^+$) transition, for example, the transition intensity was allowed to vary between the experimental limits in order not to underestimate the uncertainties in the fitted lifetime. A few transition intensities were allowed to vary with no restriction imposed, other than that they may be positive, since we could not determine their relative intensities reliably and since their internal conversion coefficients, used to obtain total intensities, are not known accurately. This was done, for example, in the case of the 60.5 keV ($9^- \rightarrow 8^+$) and the 197.3 keV ($9^- \rightarrow 7^+$) transitions. The fitted ratio of the total intensities for these two transitions is 1.9, consistent with the feeding exhibited by the data for the 926 and 789 keV transitions. This ratio agrees with other experimentally determined values but the uncertainties in these values are large owing to the experimental uncertainties.

Figure 1 is based on the level scheme given by King *et al.*[2] but has been simplified to show primarily the transitions considered in our analysis. The widths of the arrows are approximately proportional to our measured intensities. A solid arrow indicates that data for that transition were included in the fit, and lifetime results were obtained. A crosshatched arrow indicates that the transition was considered in the analysis to describe the feeding but no RDM data could be extracted. An open arrow signifies that the transition is known to occur but was not included in our analysis, either because the intensity was low enough so that it would not appreciably affect the analysis, or in order not to multiply the number of variable parameters with statistically poor data.

Figures 2 and 3 give examples of the data and typical fits to the RDM data obtained with the program PLUNGER. Typical values of reduced χ^2 for our overall fits were 1.5—2.0. The errors used for the individual data points were those propagated directly from the errors generated by the peak-fitting routine. It should be emphasized that in the final fitting procedure all of the RDM data (for every transition) are fit simultaneously. This makes

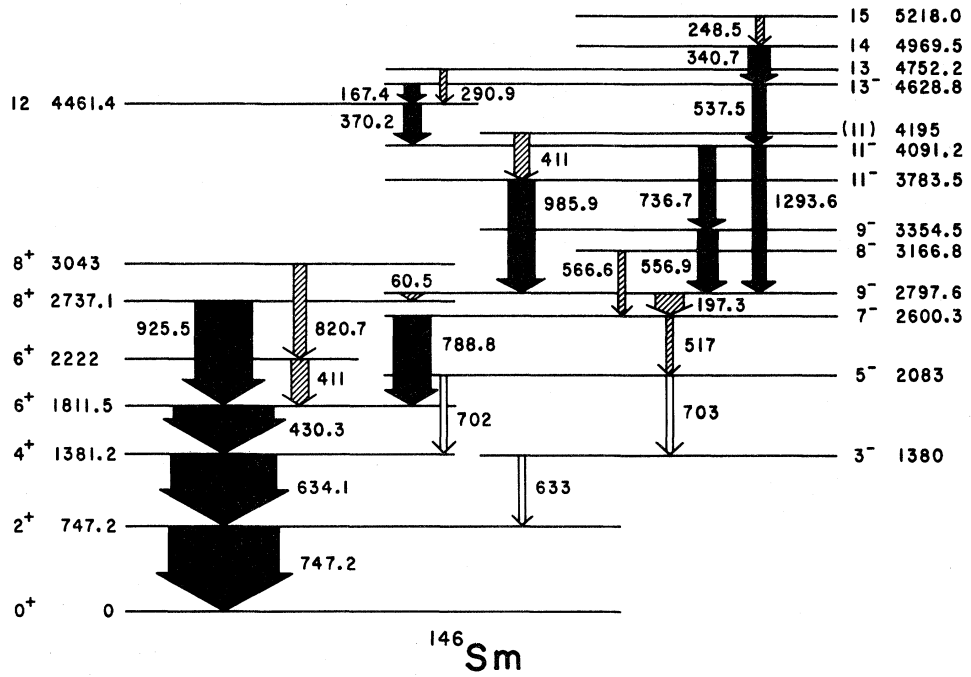

FIG. 1. Simplified decay scheme of ^{146}Sm including the gamma-ray transitions considered in the RDM analysis. Solid arrows indicate that RDM data were obtained for that transition. Crosshatched arrows indicate gamma rays which were included in analysis, but for which no RDM data were extracted. Open arrows indicate known transitions which were not included in the analysis.

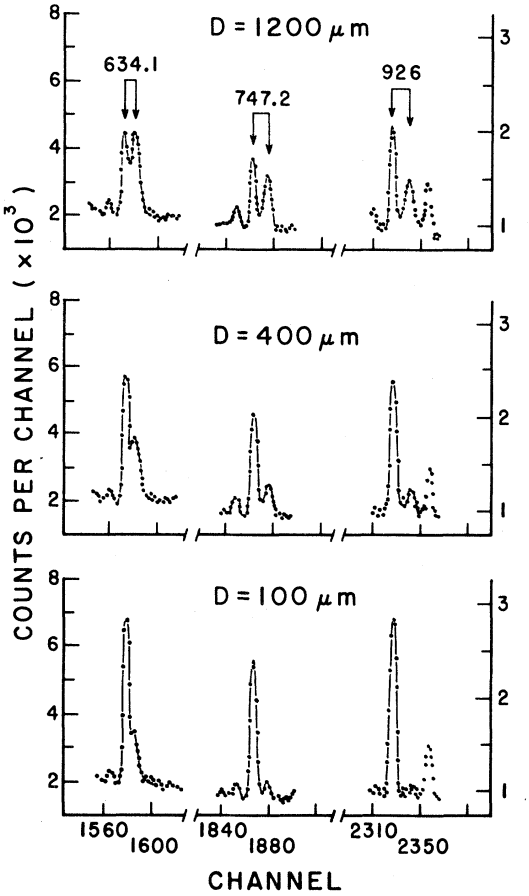

FIG. 2. Shapes of 634, 747, and 926 keV gamma-ray peaks (shifted and unshifted) at foil separation distances of 100, 400, and 1200 μm. The vertical scale on the right of the figure is for the 926 keV gamma ray only.

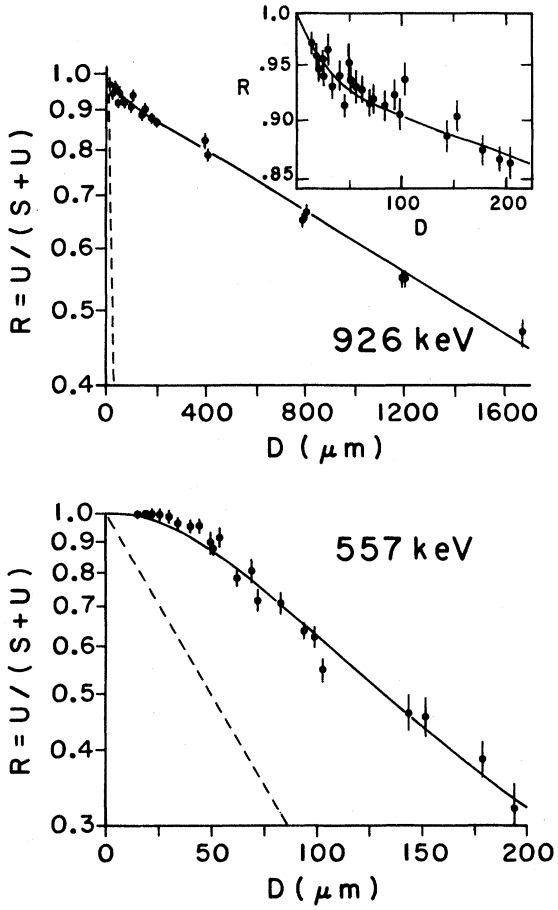

FIG. 3. Results of fits to the RDM data for the 926 and 557 keV γ rays using the program PLUNGER. The inset shows the results for the 926 keV transition for values of $D < 200$ μm. The solid curves are those generated using the lifetime values in Table I which were obtained by fitting the data for all transitions simultaneously. Those curves shown are for meanlives of 16.4 psec for the 2737 keV state depopulated by the 926 keV transition, and 39 psec for the 3355 keV state, depopulated by the 557 keV transition. The dashed lines show the expected behavior of the data for these meanlives if there were no feeding from higher-lying states.

it possible to extract lifetimes in some cases even if no RDM data for transitions directly depopulating the level of interest are available. For example, the lifetime of the long-lived level at 2798 keV is extracted primarily from the data for the 789 and 926 keV gamma transitions, and to a lesser extent from the data for the 430, 634, and 747 keV transitions. In some cases, when the feeding to a level near the top of the cascade was unknown, the RDM data were used only to parametrize the feeding to lower levels in the cascade, and no attempt was made to extract a lifetime for this higher level. Such is the case for the 341 keV transition depopulating the level at 4970 keV.

Table I presents the results of our lifetime measurements. The only previously published results are those of King *et al.*[2] who reported an upper limit of 1.5 nsec for the mean lifetime of the 9^- state at 2798 keV and Kownacki *et al.*[3] who reported an estimate of 1.0 ± 0.5 nsec for this lifetime.

We see some evidence for a mean lifetime on the order of 500 psec above the 9^- isomeric state. In fact, all the RDM data we obtained for states above the 9^- level exhibit a long-lived component to varying degrees, and the data for the 340.7 keV transition depopulating the 4969.5 keV level can be fit well, within statistical accuracy, by attributing this lifetime to the level at 5218 keV. However, we do not conclude that this is the lifetime of this level because the feeding pattern in that region of the decay

TABLE I. Measured mean lifetimes in ^{146}Sm.

Level energy (keV)	I^π	τ (psec)	Depopulating transitions (keV)
747.2	2_1^+	$7.3^{+3.0}_{-7.3}$	747.2
1381.2	4_1^+	$\sim 3\ ^{+10}_{-3}$	634.1
1811.5	6_1^+	$125\ ^{+140}_{-70}$	430.3
2600.3	7_1^-	$15.7^{+6.0}_{-6.0}$	516.8, 788.8
2737.1	8_1^+	$16.4^{+6.0}_{-6.0}$	925.5
2797.6	9_1^-	$1200\ ^{+290}_{-190}$	60.5, 197.3
3354.5	9_2^-	$38.8^{+6.5}_{-5.7}$	556.9
3783.5	11_1^-	$14.5^{+5.5}_{-4.8}$	985.9
4091.2	11_2^-	$7.1^{+2.1}_{-1.9}$	736.7, 1293.6
4461.4	12^-	$2.3^{+6.0}_{-2.3}$	370.2
4628.8	13^-	$7.6^{+3.3}_{-2.9}$	167.4, 537.5

scheme is not known and no RDM data could be extracted for the 248.5 keV transition. This raises the possibility that relatively long-lived levels not included in our analysis and not observed in our experiments feed the higher spin levels for which we have measured lifetimes. This possible side feeding was not included in our analysis because the statistical accuracy of our data prevents us from extracting such side-feeding lifetimes reliably. This is a possible source of systematic error for the higher spin states. The internal consistency of our data, however, indicates that we have reliably extracted lifetimes for levels up to at least the 11^- state at 3783.5 keV. Various estimates have been made of the magnitude of the side-feeding lifetimes (see Refs. 9–11). Measurements by the Chalk River group[11] indicate that the delays to states of spin 6–12 are typically 1–3 psec for a variety of (HI,xn) reactions. There is some indication that the side-feeding lifetimes decrease with increasing spin (see Ref. 9). There is also some evidence that the side-feeding lifetimes increase somewhat as the nuclei become more vibrational (see Ref. 10). In the case of a decay scheme like ^{146}Sm the meaning of the term "side feeding" is less clear.

Paradoxically, the data for the strongest transitions in the decay scheme [the 430.3 ($6^+\rightarrow 4^+$), 634.1 ($4^+\rightarrow 2^+$), and 747.2 ($2^+\rightarrow 0^+$) keV transitions] were difficult to fit. This is primarily due to the fact that the time behavior of these data is almost completely dominated by the feeding from the 9^- isomeric level at 2797.6 keV. An extra complication for the 430.3 keV data was that the "411 keV" transition feeding that level is a doublet with a second "411 keV" transition depopulating the 4195 keV state. Fortunately the lifetime of the 6^+ level is long enough so that its lifetime could be extracted, although with large uncertainty. The data for the 634.1 keV ($4^+\rightarrow 2^+$) transition is complicated by the fact that this gamma ray forms a doublet with the 633 keV gamma ray depopulating the 3^- state at 1380 keV. Furthermore, the 4^+ level is being fed by a 702 keV transition from the 5^- state at 2083 keV whose lifetime is unknown. The lifetime listed in the table is simply a value that gives the best fit to the data and should not be regarded much more seriously than that. The upper limit on that number, however, we feel is realistic and represents an estimate of the lifetime of the 4^+ level. The data for the 747.2 keV transition ($2^+\rightarrow 0^+$) are also dominated by feeding effects but for some reason (perhaps fortuitously) there is much less scatter in the data in the region sensitive to the lifetime of the 2^+ level ($d \lesssim 50\ \mu$m). We therefore give the same caveat for the quoted value of this lifetime as for the value for the 4^+ level, although it is possibly more reliable.

IV. DISCUSSION

The low-lying level structure in ^{146}Sm is dominated by a set of positive parity even-spin states (0^+ to 8^+) connected by $E2$ transitions which will be referred to as the "ground-state band" and a set of negative parity states, 3^-, 5^-, 7^-, 9^- (3355 keV) and 11^- (3784 keV), having a succession of spacings similar to that of the ground-state band. The latter will be referred to as the "negative-parity band."

Table II presents the reduced transition probabilities obtained from the measured lifetime for the $E2$ transitions from the ground-state-band states up to 8^+ and those members of the negative-parity band (7^-, 9^-, and 11^-) for which partial lifetimes could be reliably extracted. Also included in the table are the enhancements over the single-particle estimates and the relevent main shell model configurations from Ref. 3. The single-particle estimates were obtained from the expression

$$B(E2)_{sp}=6\times10^{-6}A^{4/3}(e^2b^2)\ .$$

It can be seen from Table II that the enhancements are on the order of ten for the transitions between the positive parity levels except for the $8^+\rightarrow6^+$ transition. It must be noted that one must be careful in interpreting the $B(E2)$ values for the $2\rightarrow0$ and $4\rightarrow2$ transitions since these are essentially lower limits due to the very large uncertainties in the lifetime measurements for the 2^+ and 4^+ states.

Even though the uncertainties are large, the $B(E2)$ values for the $2^+\rightarrow0^+$ and $4^+\rightarrow2^+$ transitions in ^{146}Sm can be compared to the values for other Sm isotopes and to measured values for ^{144}Nd. ^{144}Nd also has $N=84$ and shows a level scheme very similar to ^{146}Sm (deGeer *et al.*).[12] A prediction for the $2^+\rightarrow0^+$ transitions can be obtained from the empirical relation of Grodzins[13] which relates the energy and $B(E2)$ values for the $2^+\rightarrow0^+$ transitions in even-even nuclei over the range of the Periodic Table. The product $E_2\cdot B(E2)$ is approximately a constant except near doubly closed shells. The systematic behavior indicates that the $B(E2)$ value for the $2^+\rightarrow0^+$ transition should be approximately 0.11 e^2b^2 corresponding to a mean lifetime of 3.2 psec for the 2^+ state. This is consistent with the measured values for the 2^+ state in ^{144}Nd, 0.102 e^2b^2 (Ref. 14) and 0.088 e^2b^2 (Ref. 15). Our value of 0.048 e^2b^2 is used for comparison with theory even though it is only about half that obtained from systematics.

The measured value[16] for $B(E2;4^+\rightarrow2^+)$ in ^{144}Nd is 0.044 e^2b^2. The upper limit on our measured lifetime for the 4^+ state in ^{146}Sm gives a lower limit of $B(E2;4^+\rightarrow2^+)=0.061$ e^2b^2 which is the value also used for comparison with theory.

It is evident from Table II that the strong $E2$ transitions between negative parity levels appear to follow the same pattern as those between the ground-state band levels except for the 516.8 keV transition from the 7^- level. This last value has several possible sources of error that might account for its apparent failure to follow the pattern. The ratio of the intensities of the 516.8 and 788.8 keV gamma rays was taken from the literature,[2,3] and the spread of reported values for this ratio ranges from 0.07 to 0.12. An average value was used in the table. Another possible source of error was the fact that in our experiment the shifted and unshifted components of the 788.8 keV transition are composite with a 791 keV peak most likely originating from the decay of ^{204}Bi produced by reactions with the gold stopper and backing foils. This is conceivably a source of systematic error, which would then extend the statistical error limits on our measured value for the lifetime of the 7^- level. The composite peaks were fit in several ways with different constraining conditions on the various fitting parameters. Slightly different lifetime values were obtained from the various methods used, and the final method chosen was the one which gave the least scatter in the data points.

The fact that the negative parity band displays the same behavior as the positive parity band is an indication of the validity of the interpretation of this band as an octupole phonon coupled to the

TABLE II. Reduced transition probabilities and enhancements for $E2$ transitions from ground-state band and negative-parity band; main shell model configurations.

I^π	Transition energy (keV)	$B(E2)_{exp}$ (e^2b^2)	$\frac{B(E2)}{B(E2)_{sp}}$	Main shell model configurations (Ref. 3)	I^π	Transition energy (keV)	$B(E2)_{exp}$ (e^2b^2)	$\frac{B(E2)}{B(E2)_{sp}}$	Main shell model configurations (Ref. 3)
2_1^+	747	$0.05^{+\infty}_{-0.01}$	10[a]	$\nu(f_{7/2}^2)_{2+}\pi(d_{5/2}^{-2})_{0+}$	5_1^-				$\nu(f_{7/2}i_{13/2})_{5-}\pi(d_{5/2}^{-2})_{0+}$
4_1^+	634	≥0.061	≥13[a]	$\nu(f_{7/2}^2)_{4+}\pi(d_{5/2}^{-2})_{0+}$	7_1^-	517	$0.013^{+0.010}_{-0.005}$	3[b]	$\nu(f_{7/2}i_{13/2})_{7-}\pi(d_{5/2}^{-2})_{0+}$
6_1^+	430	$0.04^{+0.06}_{-0.02}$	9.6	$\nu(f_{7/2}^2)_{6+}\pi(d_{5/2}^{-2})_{0+}$	9_1^-	197	$0.05^{+0.01}_{-0.01}$	11.6[b]	$\nu(f_{7/2}i_{13/2})_{9-}\pi(d_{5/2}^{-2})_{0+}$
8_1^+	926	$0.0073^{+0.0004}_{-0.0002}$	1.6	$\nu(f_{7/2}h_{9/2})_{8+}\pi(d_{5/2}^{-2})_{0+}$	11_1^-	986	$0.006^{+0.003}_{-0.002}$	1.3	$\nu(h_{9/2}i_{13/2})_{11-}\pi(d_{5/2}^{-2})_{0+}$

[a] See text for discussion.

[b] To deduce partial lifetimes for relevant transitions, ratios of intensities were taken from the literature and averaged. Internal conversion coefficients were taken from Ref. 1.

ground-state band. This was suggested by the energy spacings and was pointed out by King *et al.*[2]

The $B(E1)$ values for the two $E1$ transitions of 788.8 keV ($7^- \rightarrow 6^+$) and 60.5 keV ($9^- \rightarrow 8^+$) which proceed between the negative parity band and the ground band are 7.4×10^{-7} and 8.2×10^{-6} e^2b, respectively. The retardation factors are about 2×10^3 and 2×10^4, respectively, and are fairly typical for the $E1$ transitions of this type.

The behavior of the positive parity band can be somewhat understood if one considers the most likely dominant shell model configurations which are tabulated in Table II. The positive parity levels up to 6^+ have the same basic quasiparticle configurations. However, the 8^+ level probably has a different configuration for the neutrons. The negative parity band follows this pattern but with one $f_{7/2}$ neutron replaced by an $i_{13/2}$ neutron. The single-particle transition strength for the 8^+ to 6^+ transition and for the 11^- to 9^- transition can then be understood qualitively as being dominated by the change in the quasiparticle configuration of the neutrons. The factor of 10 enhancement of the other transitions indicates some collective nature for these transitions. A qualitative difference between the 8^+ state and the other states in the band is also indicated by the large value for the 8^+-6^+ level spacing compared to the other spacings for the lower transitions (a similar effect is seen for the negative parity states). These characteristics indicate that an appropriate model to describe the observed behavior might be the cluster-vibrator model (CVM) which couples single-particle degrees of freedom to collective excitations of the core.[17]

Figure 4 and Table III present our experimental data compared to model calculations. The CVM wave functions used are those from Refs. 2 (King *et al.*) and 4 (Van den Berghe). The calculations are approximate since the wave functions listed in these references are not complete but only present the components that contribute more than 4% to the total wave function. The wave functions were renormalized and the variable parameters were not adjusted but were taken directly from Ref. 4. This procedure reproduced well the calculated electromagnetic properties given in Ref. 4 and significant error is not introduced by using truncated wave functions. The CVM calculations appear to reproduce the trends in the data well, except for the $8^+ \rightarrow 6^+$ transition. The disagreement for the 8^+ level is probably not significant since the wave functions were deduced primarily from level spacing with little data on transition probabilities being available. The author of Ref. 4 states his reservations about the 8^+ wave function.

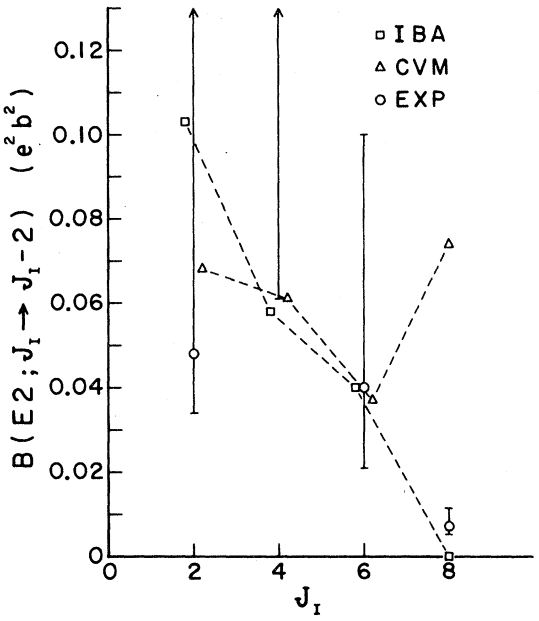

FIG. 4. Comparison of experimental $B(E2)$ values for the ground-state band in ^{146}Sm with predictions from the CVM and IBA models.

Also in Fig. 4 are presented calculations carried out using the interacting-boson approximation.[5,18,19] The motivation for doing this is questionable since the IBA model is essentially a description of collective phenomena and should not be expected to work

TABLE III. Comparison of experimental and theoretical $B(E2)$ values.

I^π	Transition energy (keV)	$B(E2)_{exp}$ (e^2b^2)	$B(E2)_{CVM}$ (e^2b^2)	$B(E2)_{IBA}$ (e^2b^2)
2_1^+	747.2	$0.048^{+\infty}_{-0.01}$ [a]	0.068	0.103
4_1^+	634.1	≥ 0.061 [a]	0.061	0.058
6_1^+	430.3	$0.04^{+0.06}_{-0.02}$	0.037	0.040
8_1^+	925.5	$0.007^{+0.004}_{-0.002}$	0.074	1.6×10^{-5}

[a] See text for discussion.

very well close to the $N=82$ closed shell. In fact the model has been shown to be equivalent to a drastic reduction in the available shell model space and thus should not be expected to contain all the quasiparticle degrees of freedom of the positive parity levels (see Refs. 20 and 21). However, ^{146}Sm was one of the nuclei examined in a systematic study of the Sm isotopes reported in Refs. 18 and 19. The model predicts fairly well the positions of the positive parity levels in ^{146}Sm at least up to 6^+. It is interesting to see how well it can do for the electromagnetic properties as well. We have varied the IBA parameters to better reproduce the positions of known levels in ^{146}Sm and the results for the ground state band are given in Table IV. The version of the IBA model used makes no distinction between neutron and proton bosons.

The agreement between the data and the model calculations is quite good at least up the 6^+ level. There is a substantial disagreement for the 8^+-6^+ transition, with the $B(E2)$ value being significantly smaller than the experimental value. It is even much smaller than the single-particle estimate

$$[B(E2);\nu(h_{9/2}f_{7/2})_{8+}\rightarrow\nu(f_{7/2}{}^2)_{6+}]$$
$$=1.3\times10^{-4}\ e^2\mathrm{b}^2\ ,$$

(assuming the configuration given, an effective charge of 0.5 e and harmonic oscillator estimates for the radial integrals). This indicates that a large portion of the wave function of the 8^+ state contains configurations not included in the truncated shell model space considered by the model. It is interesting that none of the simple limiting cases of the IBA model [SU(5): anharmonic vibrator; SU(3): axial rotor; O(6): γ-unstable limit] predict a reduction in the $B(E2)$ strength in the ground-state band with increasing spin.

Kownacki *et al.*[3] disagree with King *et al.*[2] on the parity assignment for the 4628.8 ($I=13$) and 4461.4 ($I=12$) keV levels. King *et al.* assigned negative parity to the 4628.8 keV level, presumably on the basis of the quadrupole character of the 537.5 keV transition as determined from the angular distribution data. They do not assign a parity for the 4461.4 keV level but the placement in their decay scheme would favor positive parity. Kownacki *et al.*[3] assign negative parity to the 4461.4 keV level and positive parity to the 4628.8 keV level based on internal conversion coefficient measurements for the 370.2 and 167.4 keV transitions which indicate $M1$ and $E1$, respectively. They see no evidence for the 537.5 keV transition.

In our experiment both the 537.5 and 167.4 keV transitions are observed. The region of the spectrum around the 167.4 keV full energy peak was relatively clean and the method of peak fitting allowed the extraction of RDM data for this transition even though the shifted and unshifted full energy peaks were not resolved. The errors on these data are understandably large; however, the time behavior agrees well with that for the 537.5 keV data as seen in Fig. 5. The curves drawn through the points result from the fit to the RDM data assuming that both gamma rays depopulate the 4628.8 keV level. These data and the fact that the 537.5 keV transition fits energetically between the 4628.8 and 4091.2 keV levels strongly indicate that the placement by King *et al.* is correct.

On the basis of the angular distribution data of King *et al.*[2] one may conclude that the 4091.2 keV level is 11^- and the 537.5 keV transition is quadrupole. Our lifetime data for the 4628.8 keV state strongly favor $E2$ character for this 537.5 keV transition with an enhancement factor of about 20, suggesting some collective nature. Thus the spin parity of the 4628.8 keV state is most likely 13^- and the 167.4 and 370.2 keV transitions must both be $E1$ or both $M1+E2$. If they are both $E1$ then the 370.2 keV internal conversion results of Kownacki *et al.* are in error, whereas if they are of $M1+E2$ character then the 167.4 keV results are incorrect. The latter is more likely since they do not observe the 537.5 keV gamma ray, suggesting that the 167.4

TABLE IV. Comparison of level energies from IBA calculation and experiment.

I^π	Energy$_{exp}$ (keV)	Energy$_{IBA}$ (keV)[a]	ΔE (keV)
2_1^+	747.2	753.3	−6.1
4_1^+	1381.2	1382.2	−1.0
6_1^+	1811.5	1961.7	−150.2
8_1^+	2737.1	2785.8	−48.7

[a]IBA parameters; HBAR $=1.212$, $F=0.1755$, $G=-0.1858$, $C_0=-0.2452$, $C_2=-0.5590$, $C_4=-0.1814$, $E2SD=0.08727$, $E2DD=-0.2355$.

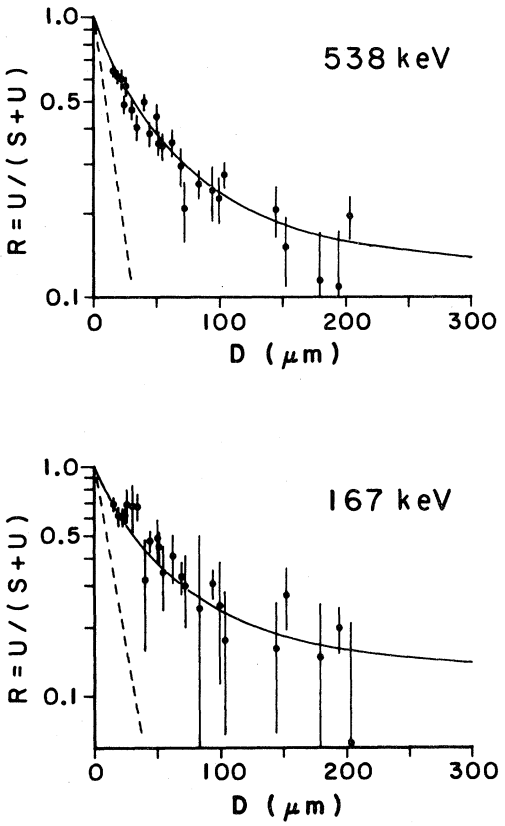

FIG. 5. Results of fits to the RDM data for the 167 and 538 keV γ rays using the program PLUNGER, assuming that both transitions depopulate the same state.

keV gamma ray they did observe may have another origin. Furthermore, if the 167.4 and 370.2 keV transitions are $E1$ one obtains hindrance factors of $\simeq 150$ and 350 from our lifetime data. These would be small compared to $E1$ hindrance factors normally observed. (The 60.5 and 788.8 keV $E1$ transitions have hindrance factors of $\simeq 2\times 10^3$ and 2×10^4.) If the 167.4 and 370.2 keV transitions are $M1$ the partial γ-ray lifetimes are slightly greater than those obtained from single-particle estimates.

We thus conclude that the most likely assignments for the 4461.4 and 4628.8 keV states are 12^- and 13^-. It is interesting to note that these assignments are consistent with the suggestion of Peker and Tuli[22] that these states may be members of a strongly-coupled rotational band built on the 11^- state at 4091.2 keV. They also suggest similar bands in other $N=84$ nuclei.

The lifetime data for the intense 736.7 and 1293.6 keV transitions depopulating the 4091.2 keV (11_2^-) state should help in evaluating this possible interpretation. Our results give a partial γ-ray lifetime $\tau_\gamma \cong 10$ psec for the 1293.6 keV $E2$ transition to the 9_1^- state at 2797.6 keV (retardation $\cong 5$) and $\tau_\gamma \cong 24$ psec for the 736.7 keV $E2$ transition to the 9_2^- state at 3354.5 keV (enhancement $\cong 8$).

In conclusion we can state that our lifetime measurements support the proposed quasiparticle structure for the ground-state band up to 8^+. They also support the interpretation of the negative parity levels from 3^- up to 11^- as a coupling of an octupole phonon to the ground state band. Both the CVM and IBA models appear to describe adequately the ground-state band up to and including the 6^+ level. Both fail to describe the $B(E2)$ value of the 8^+-6^+ transition. In the case of the CVM a recalculation with new information may help the agreement. We have also shown how RDM measurements of this kind can be used to resolve spin and parity ambiguities.

ACKNOWLEDGMENTS

The authors wish to thank Dr. R. Kaczarowski and Dr. P. R. Chagnon for helpful discussions, and Dr. D. Rakel for his assistance. This work was supported in part by the National Science Foundation, Grant No. PHY 80-08234.

APPENDIX A: ALGORITHM FOR CASCADE FEEDING

In the subsequent discussion the following definitions and conventions are used:

(1) Levels are numbered consecutively in order of increasing energy starting with 1 for the lowest and so on up to the topmost level. Transitions to levels not included in the part of the decay scheme being analyzed are said to terminate at level 0 for bookkeeping purposes.

(2) λ_j is the decay constant of level j.

(3) I_m^k is the relative total transition intensity (including internal conversion) for the transitions from level m to level k.

(4) The total decay intensity of transitions depopulating level m is I_m, where

$$I_m \equiv \sum_{j=0}^{m-1} I_m^j \ .$$

The total decay intensity of transitions populating level m is I^m, where

$$I^m \equiv \sum_{j=m+1}^{n} I_j^m \ .$$

(5) N_k is the direct populating intensity of level k either by decay from the compound nucleus or by any fast populating mechanism. Normally N_k is taken to be

$$N_k = I_k - I^k .$$

With the above definitions, the population of a level, indexed by k, can be written as

$$P_k(t) = \sum_{j=k}^{n} a_j^k e^{-\lambda_j t} .$$

Similarly the ratio R_k for the same level (ignoring higher-order corrections) can be written as

$$R_k(t) = \sum_{j=k}^{n} b_j^k e^{-\lambda_j t} ,$$

with the following expressions for the coefficients a_j^k and b_j^k,

$$a_j^k = 0 \text{ for } j < k, \quad j > n ,$$

$$a_j^k = \sum_{m=k+1}^{j} \frac{I_m^k}{I_m} \frac{a_j^m \lambda_m}{\lambda_k - \lambda_j} ,$$

$$a_k^k = N_k - \sum_{j=k+1}^{n} a_j^k ,$$

$$b_j^k = \frac{a_j^k/\lambda_j}{\sum_{m=k}^{n} a_m^k/\lambda_m} .$$

The coefficients a_j^k must be calculated for the highest level first and so on down. This algorithm can be used with any decay scheme no matter how complicated and the only assumption used in this derivation is that the populations of each must satisfy the conventional expression for nuclear decay.

APPENDIX B: TARGET ALIGNMENT USING A LASER

A method of aligning the target and stopper foils was devised that was both sensitive and faster than the method employed previously, namely examining the foil separation under a microscope, with backlighting used to highlight the separation gap. By reflecting a laser beam off the foils, one has an optical lever which magnifies the relative angle between the stopper and target foils. The principle is illustrated schematically in Fig. 6. By a suitable choice of target-to-screen distance and angle of incidence

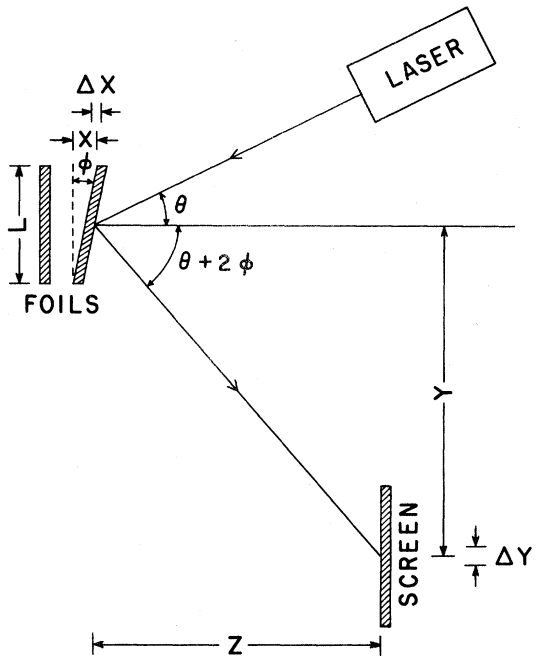

FIG. 6. Schematic illustration of the foil alignment technique using an optical lever.

one can achieve a magnification of several thousand. Specifically, the magnification is given by the following expression

$$M = \frac{dy}{dx} = \frac{2z}{L}(1 + y^2/z^2) .$$

The procedure used is described below. The plunger apparatus was clamped in a firm support, and the stopper foil was then mounted. The laser beam was reflected off its front face (the side facing the target foil) and the position of the reflected beam spot was noted on the screen. Each of the foil holders can be rotated about only one axis which is perpendicular to that of the other foil holder. The target foil was then mounted and the holder was rotated about a horizontal axis until the reflected beam was at the same vertical level as the previous spot. The target foil was then removed and the stopper foil was rotated about the vertical axis until the reflected spot was on the same vertical line as the previous spot. This procedure was repeated until the two reflected beam spots were coincident. With practice this method allowed one to align the foils in about five to ten minutes with results comparable to, and usually better than, results using a microscope.

To get the same magnification in both the verti-

cal and horizontal directions the laser beam must make the same incident angle when projected onto the planes perpendicular to the foil faces and their axes of rotation. The magnification which we usually achieved was about 2000 in the horizontal direction and 1000 in the vertical.

The quality of the reflected beam spot is dependent largely on the quality of the foil, and gold and nickel foils gave comparably good results. The backing on the target foils almost always gave a poorer quality reflected spot than did the stopper foils probably due to the fact that target foils were subjected to additional stresses during the evaporation process when the target material was deposited. The irregularities in the reflected beam spot were consistent with surface irregularities.

---

*Present address: U. S. Nuclear Regulatory Commission, Glen Ellyn, Illinois.

[1]B. Singh and M. W. Johns, Can. J. Phys. 53, 391 (1975).
[2]C. H. King, B. A. Brown, and T. L. Khoo, Phys. Rev. C 18, 2127 (1977).
[3]J. Kownacki, Z. Sujkowski, E. Hammaren, E. Liukkonen, M. Piiparinen, Th. Lindblad, H. Ryde, and V. Paar, Nucl. Phys. A337, 464 (1980).
[4]G. Van den Berghe, Z. Phys. 272, 245 (1975).
[5]A. Arima and F. Iachello, Phys. Rev. Lett. 35, 1069 (1975).
[6]S. Rozak, PLUNGER computer program, University of Notre Dame (unpublished).
[7]F. James and M. Roos, Comput. Phys. Commun. 10, 343 (1975).
[8]A. E. Blaugrund, Nucl. Phys. 88, 501 (1966).
[9]A. Faessler and M. Wakai Kernforschungsanlage Julich, Institute for Nuclear Physics, Annual Report, 1979, Sec. 5.11.
[10]J. O. Newton, F. S. Stephens, and R. M. Diamond, Nucl. Phys. A210, 19 (1973).
[11]D. Ward, in *Proceedings of the International Conference on Reactions between Complex Nuclei,* edited by R. L. Robinson, F. K. McGowan, J. B. Ball, and J. H. Hamilton (North-Holland, New York, 1974), Vol. 2, p. 417.
[12]L. E. DeGeer, A. Kerek, Z. Haratym, J. Kownacki, and J. Ludziejewski, Nucl. Phys. A259, 399 (1976).
[13]L. Grodzins, Phys. Lett. 2, 88 (1962).
[14]P. A. Crowley, J. R. Kerns, and J. X. Saladin, Phys. Rev. C 3, 2049 (1971).
[15]S. Raman. Nucl. Data B2, 47 (1967).
[16]A. Li-Scholz and H. Bakhru, Phys. Rev. C 6, 353 (1972).
[17]V. Paar, in *Problems of Vibrational Nuclei,* edited by G. Alaga, V. Paar, and L. Sips (North Holland, Amsterdam, 1975), p. 15.
[18]O. Scholten, F. Iachello, and A. Arima, Ann. Phys. (N.Y.) 115, 325 (1978).
[19]O. Scholten, thesis, Free University of Groningen, 1980.
[20]T. Otsuka, A. Arima, and F. Iachello, Nucl. Phys. A309, 1 (1978).
[21]T. Otsuka, A. Arima, F. Iachello, and I. Talmi, Phys. Lett. 76B, 139 (1978).
[22]L. K. Peker and J. K. Tuli, *Conference on Band Structure and Nuclear Dynamics* (Tulane University, Louisiana, 1980).